

PAPER

Joint Tx/Rx MMSE Filtering for Single-Carrier MIMO Eigenmode Transmission Using Iterative Interference Cancellation

Shinya KUMAGAI^{†a)}, Student Member and Fumiyuki ADACHI[†], Fellow

SUMMARY In this paper, we propose a new joint transmit and receive spatial/frequency-domain filtering for single-carrier (SC) multiple-input multiple-output (MIMO) eigenmode transmission using iterative interference cancellation (IC). Iterative IC is introduced to a previously proposed joint transmit and receive spatial/frequency-domain filtering based on minimum mean square error criterion (called joint Tx/Rx MMSE filtering) to reduce the residual inter-symbol interference (ISI) after the Rx filtering. The optimal Tx/Rx filters are derived based on the MMSE criterion taking into account the iterative IC. The superiority of our proposed technique is confirmed by computer simulation.

key words: single-carrier, MIMO, eigenmode, spatial/frequency filtering, iterative interference cancellation

1. Introduction

Multiple-input multiple-output (MIMO) [1] is a powerful technique to increase the transmission data rate without widening the signal bandwidth. MIMO with orthogonal frequency-division multiplexing (OFDM) [2], [3] is known for its robustness against frequency-selective fading [4]. However, the disadvantage of OFDM is its high peak-to-average power ratio (PAPR) of the transmit signal [3], [5].

MIMO with single-carrier (SC) block transmission [6]–[9] has been attracting much attention as an alternative technique because of its low PAPR property [7]. SC-MIMO suffers not only from inter-antenna interference (IAI) caused by MIMO multiplexing but also from inter-symbol interference (ISI) caused by severe frequency-selectivity of the channel. Minimum mean square error based linear receive spatial/frequency-domain filtering (called Rx MMSE filtering) [6], [7] achieves a good transmission performance while it is computationally efficient. However, its performance improvement is limited due to the existence of residual IAI and ISI after the filtering.

Recently, we proposed an MMSE based linear joint transmit/receive spatial/frequency-domain filtering (called joint Tx/Rx MMSE filtering) for SC-MIMO transmission [10]. Channel state information (CSI) is required at both transmitter and receiver. Joint Tx/Rx MMSE filtering transforms MIMO channel to multiple orthogonal channels (i.e., eigenmodes) to remove IAI and applies MMSE based frequency-domain Tx power allocation and Rx frequency-

domain equalization (FDE) to each eigenmode to suppress ISI. As a consequence, joint Tx/Rx MMSE filtering achieves better transmission performance than Rx MMSE filtering.

The frequency-domain Tx power allocation and Rx FDE of joint Tx/Rx MMSE filtering are designed based on MMSE criterion. Therefore, unlike zero-forcing criterion, the filtering cannot remove ISI completely but tries to suppress the impacts of both ISI and noise. As a consequence, joint Tx/Rx MMSE filtering still suffers from the residual ISI on each eigenmode. Iterative interference cancellation (IC) or iterative block decision-feedback equalizer (IB-DFE) [11]–[13] is effective to reduce the residual interference and its introduction to SC-MIMO transmission with Rx MMSE filtering was studied in [7], [8]. The residual IAI and ISI replicas are generated using the bit log-likelihood ratio (LLR) of the received signal after channel decoding and are subtracted from the received signal after Rx MMSE filtering. A sequence of Rx MMSE filtering, IC, and channel decoding is repeated for a sufficient number of times. As a consequence, the residual IAI and ISI can be suppressed well and the SC-MIMO transmission performance will be improved.

In this paper, we propose a new joint Tx/Rx MMSE filtering for SC-MIMO transmission using iterative IC and newly derive the optimal Tx/Rx filters taking into account the iterative IC at the receiver. The new joint Tx/Rx MMSE filtering transforms MIMO channel into eigenmodes to remove IAI as does previously proposed joint Tx/Rx MMSE filtering [10]. However, unlike the previous one, it applies MMSE based frequency-domain Tx power allocation and Rx FDE to each eigenmode to further suppress the residual ISI taking into account the iterative IC. Computer simulation results show that the new joint Tx/Rx MMSE filtering can significantly improve the average bit error rate (BER) performance of turbo coded SC-MIMO transmission using iterative IC.

The remainder of this paper is organized as follows. Section 2 presents the transmission system model and signal representation for SC-MIMO transmission using iterative IC with joint Tx/Rx MMSE filtering. Section 3 presents the derivation of optimal Tx/Rx filters based on MMSE criterion and discusses their behavior. In Sect. 4, we evaluate the average BER performance achievable with the proposed technique by computer simulation. Section 5 gives the concluding remarks.

Notations: $E[\cdot]$, $\text{tr}[\cdot]$, $[\cdot]^T$, and $[\cdot]^H$ denote ensemble average operation, trace operation, transpose operation, and

Manuscript received March 31, 2015.

Manuscript revised August 3, 2015.

[†]The authors are with the Department of Communications Engineering, Graduate School of Engineering, Tohoku University, Sendai-shi, 980-8579 Japan.

a) E-mail: kumagai@mobile.ecei.tohoku.ac.jp

DOI: 10.1587/transcom.2015EBP3136

Hermitian transpose operation, respectively. $(x)^\dagger$ denotes $\max(0, x)$. \mathbf{I}_N is the $N \times N$ identity matrix and $\mathbf{0}_{N \times M}$ is the $N \times M$ zero-matrix.

2. SC-MIMO Transmission Using Iterative IC with Joint Tx/Rx MMSE Filtering

In this paper, we use a symbol-spaced discrete-time signal representation. The system model of SC-MIMO transmission using iterative IC with joint Tx/Rx MMSE filtering is illustrated in Fig. 1. A transmitter and a receiver have N_t and N_r antennas, respectively. For the sake of brevity, we assume $N_t \leq N_r$.

In this paper, we assume a time-division duplex (TDD) transmission. In TDD transmissions, the transmitter can reuse the CSI which was estimated in the previous time slot (i.e., when the transmitter was operated as a receiver). Therefore, the CSI can be shared among the transmitter and receiver at the present time slot in low mobility environment or with accurate channel prediction methods. The impact of channel estimation error is left as an interesting future work.

2.1 Transmit Signal

At the transmitter, two parity bit sequences generated by turbo encoding are punctured to form the codeword of length K . The codeword is interleaved, serial-to-parallel (S/P) converted to N_t parallel bit streams, and then each stream is data-modulated. Each symbol stream is divided to N_c -symbol blocks, where N_c is the size of discrete Fourier transform (DFT) and inverse DFT (IDFT), and each data symbol block $\{d_n(t); t=1 \sim N_c\}$, $n=1 \sim N_t$, is transformed into a frequency-domain data symbol block $\{D_n(k); k=1 \sim N_c\}$, $n=1 \sim N_t$, by N_c -point DFT. The transmit symbol vector $\mathbf{S}(k)=[S_1(k) \cdots S_{N_t}(k)]^T \in \mathbb{C}^{N_t \times 1}$ at the k -th frequency is obtained by applying the Tx MMSE filtering to the frequency-

domain data symbol vector $\mathbf{D}(k)=[D_1(k) \cdots D_{N_t}(k)]^T \in \mathbb{C}^{N_t \times 1}$, which is expressed as

$$\mathbf{S}(k) = \mathbf{W}_t(k)\mathbf{D}(k), \quad (1)$$

where $\mathbf{W}_t(k) \in \mathbb{C}^{N_t \times N_t}$ is the Tx filter matrix. N_c -point IDFT is applied to each transmit symbol block $\{S_n(k); k=1 \sim N_c\}$, $n=1 \sim N_t$, to transform back to time-domain transmit blocks. Finally, the last N_g symbols of each transmit block are copied as a cyclic prefix (CP) and inserted into the guard interval (GI) at the beginning of each transmit block and then transmitted from N_t antennas.

2.2 Received Signal

At the receiver, after removing CP, the superimposed signal block received by each of N_r antennas is transformed into the frequency-domain signal by N_c -point DFT. The frequency-domain received signal vector $\mathbf{R}(k) \in \mathbb{C}^{N_r \times 1}$ at the k -th frequency after N_c -point DFT is expressed as

$$\mathbf{R}(k) = \sqrt{\frac{2E_s}{T_s}}\mathbf{H}(k)\mathbf{S}(k) + \mathbf{Z}(k), \quad (2)$$

where E_s and T_s are the average transmit symbol energy and symbol duration, respectively. $\mathbf{H}(k) \in \mathbb{C}^{N_r \times N_t}$ is the MIMO channel matrix and $\mathbf{Z}(k) \in \mathbb{C}^{N_r \times 1}$ is the noise vector whose elements are zero-mean complex-valued random variables having the identical variance $2N_0/T_s$ with N_0 being the one-sided power spectrum density of additive white Gaussian noise (AWGN).

Iterative Rx filtering & IC is applied to $\mathbf{R}(k)$. Let us consider the i ($=1 \sim I$)-th iteration stage, where I denotes the number of outer loop (between Rx filtering and turbo decoding) iterations. Only Rx filtering (i.e., without IC) is applied at the receiver at the $i=1$ st iteration stage. The frequency-domain soft-output vector $\hat{\mathbf{R}}^{(i)}(k) \in \mathbb{C}^{N_r \times 1}$ is obtained by performing the Rx MMSE filtering on $\mathbf{R}(k)$ as

$$\begin{aligned} \hat{\mathbf{R}}^{(i)}(k) &= \mathbf{W}_r^{(i)}(k)\mathbf{R}(k) \\ &= \sqrt{\frac{2E_s}{T_s}}\tilde{\mathbf{H}}^{(i)}\mathbf{D}(k) \\ &\quad + \sqrt{\frac{2E_s}{T_s}}(\mathbf{W}_r^{(i)}(k)\mathbf{H}(k)\mathbf{W}_t(k) - \tilde{\mathbf{H}}^{(i)})\mathbf{D}(k) \\ &\quad + \mathbf{W}_r^{(i)}(k)\mathbf{Z}(k), \end{aligned} \quad (3)$$

where $\mathbf{W}_r^{(i)}(k) \in \mathbb{C}^{N_r \times N_r}$ is the Rx filter matrix at the i -th iteration. $\tilde{\mathbf{H}}^{(i)} \in \mathbb{C}^{N_r \times N_t}$ is the diagonal matrix whose (n, n) -th component is the equivalent channel gain $\tilde{H}_n^{(i)}$ of the desired signal after joint Tx/Rx MMSE filtering. $\tilde{H}_n^{(i)}$ is expressed as

$$\tilde{H}_n^{(i)} = \frac{1}{N_c} \sum_{k=1}^{N_c} \sum_{m=1}^{N_r} W_{r,n,m}^{(i)}(k) \sum_{n'=1}^{N_t} H_{m,n'}(k) W_{t,n',n}(k), \quad (4)$$

where $W_{r,n,m}^{(i)}(k)$, $H_{m,n'}(k)$, and $W_{t,n',n}(k)$ are the (n, m) -th component of $\mathbf{W}_r^{(i)}(k)$, (m, n') -th component of $\mathbf{H}(k)$, and

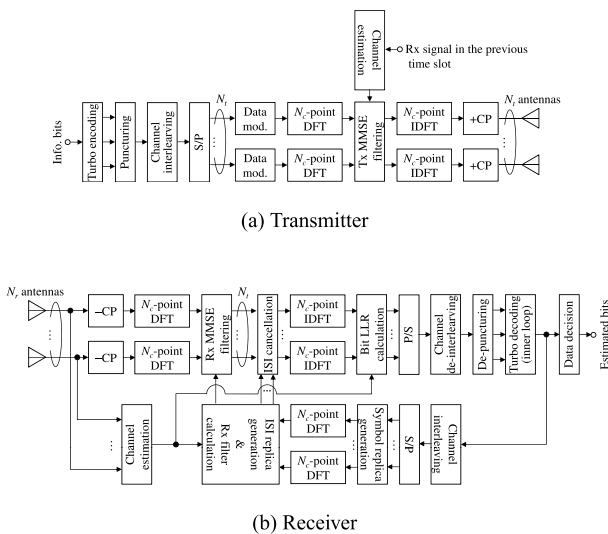


Fig. 1 System model of SC-MIMO transmission using iterative IC with joint Tx/Rx MMSE filtering.

(n', n) -th component of $\mathbf{W}_r(k)$, respectively. In the right side of Eq. (3), the first, second, and third terms are the desired signal, residual ISI after joint Tx/Rx filtering, and noise, respectively.

In order to suppress the residual ISI expressed as the second term of the right side of Eq. (3), the residual ISI replica is generated using the frequency-domain soft-output data symbol replica vector $\tilde{\mathbf{D}}^{(i-1)}(k) \in \mathbb{C}^{N_c \times 1}$ at the previous (i.e., $(i-1)$ -th) iteration stage, and is subtracted from $\hat{\mathbf{R}}^{(i)}(k)$. For the first iteration stage (i.e., $i=1$), $\tilde{\mathbf{D}}^{(0)}(k) = \mathbf{0}_{N_c \times 1}$. $\tilde{\mathbf{D}}^{(i-1)}(k)$ for $i > 1$ will be presented in Sect. 2.4. The frequency-domain soft-output vector $\hat{\mathbf{D}}^{(i)}(k) \in \mathbb{C}^{N_c \times 1}$ after the IC is expressed as

$$\begin{aligned} \hat{\mathbf{D}}^{(i)}(k) &= [\hat{D}_1(k) \cdots \hat{D}_{N_c}(k)]^T \\ &= \hat{\mathbf{R}}^{(i)}(k) - \sqrt{\frac{2E_s}{T_s}} (\mathbf{W}_r^{(i)}(k) \mathbf{H}(k) \mathbf{W}_t(k) - \tilde{\mathbf{H}}^{(i)}) \tilde{\mathbf{D}}^{(i-1)}(k) \\ &= \sqrt{\frac{2E_s}{T_s}} \tilde{\mathbf{H}}^{(i)} \mathbf{D}(k) \\ &+ \sqrt{\frac{2E_s}{T_s}} (\mathbf{W}_r^{(i)}(k) \mathbf{H}(k) \mathbf{W}_t(k) - \tilde{\mathbf{H}}^{(i)}) (\mathbf{D}(k) - \tilde{\mathbf{D}}^{(i-1)}(k)) \\ &+ \mathbf{W}_r^{(i)}(k) \mathbf{Z}(k). \end{aligned} \quad (5)$$

N_c -point IDFT is applied to each frequency-domain soft-output block $\{\hat{D}_n^{(i)}(k); k=1 \sim N_c, n=1 \sim N_t\}$. Then, the time-domain soft-output vector $\{\hat{\mathbf{d}}^{(i)}(t) = [\hat{d}_1^{(i)}(t) \cdots \hat{d}_{N_t}^{(i)}(t)]^T \in \mathbb{C}^{N_t \times 1}; t=1 \sim N_c\}$ is obtained.

2.3 Turbo Decoding

Turbo decoding is carried out using the bit LLRs obtained from $\hat{\mathbf{d}}^{(i)}(t)$. The bit LLR $\lambda_n^{(i)}(t, x)$ corresponding to the $x(=1 \sim \log_2 M)$ -th bit of $d_n(t)$ after the IC at the i -th iteration stage is calculated as

$$\begin{aligned} \lambda_n^{(i)}(t, x) &\approx \frac{\left| \hat{d}_n^{(i)}(t, x) - \sqrt{\frac{2E_s}{T_s}} \tilde{H}_n^{(i)} d_{b_n(t,x)=0}^{\min} \right|^2}{2\{\sigma_n^{(i)}\}^2} \\ &- \frac{\left| \hat{d}_n^{(i)}(t, x) - \sqrt{\frac{2E_s}{T_s}} \tilde{H}_n^{(i)} d_{b_n(t,x)=1}^{\min} \right|^2}{2\{\sigma_n^{(i)}\}^2}, \end{aligned} \quad (6)$$

where M is the modulation level. $b_n(t, x)$ is the x -th bit of $d_n(t)$. $d_{b_n(t,x)=0}^{\min}$ or $d_{b_n(t,x)=1}^{\min}$ are the most probable symbols which give the minimum Euclidean distance from $\hat{d}_n^{(i)}(t)$ among all candidate symbols with $b_n(t, x)=0$ or 1. $2\{\sigma_n^{(i)}\}^2$ is the variance of the residual ISI plus noise of the n -th data streams at the i -th iteration which is expressed as

$$\begin{aligned} 2\{\sigma_n^{(i)}\}^2 &= \frac{2E_s}{T_s} \rho_n^{(i-1)} \left\{ \frac{1}{N_c} \sum_{k=1}^{N_c} |\hat{H}_n^{(i)}(k)|^2 - \tilde{H}_n^{(i)} \right\} \\ &+ \frac{2N_0}{T_s N_c} \sum_{k=1}^{N_c} \sum_{m=1}^{N_t} |W_{r,n,m}^{(i)}(k)|^2, \end{aligned} \quad (7)$$

where $\rho_n^{(i-1)}$ represents the mean square error between the data symbol and the symbol replica as

$$\begin{aligned} \rho_n^{(i-1)} &= E \left[|d_n(t) - \tilde{d}_n^{(i-1)}(t)|^2 \right] \\ &\approx \begin{cases} \frac{1}{N_c} \sum_{k=1}^{N_c} \left\{ 1 - |\tilde{d}_n^{(i-1)}(t)|^2 \right\} & \text{for QPSK,} \\ \frac{1}{N_c} \sum_{k=1}^{N_c} \left\{ \frac{4}{10} \tanh \left(\frac{\hat{\lambda}_n^{(i-1)}(t, 2)}{2} \right) \right. \\ \quad \left. + \frac{4}{10} \tanh \left(\frac{\hat{\lambda}_n^{(i-1)}(t, 4)}{2} \right) + 1 - |\tilde{d}_n^{(i-1)}(t)|^2 \right\} & \text{for 16QAM,} \end{cases} \end{aligned} \quad (8)$$

for $i > 1$, and $\rho_n^{(0)} = 1$ for $i=1$. $\tilde{d}_n^{(i-1)}(t)$ is the time-domain soft-output data symbol replica of $d_n(t)$ at the $(i-1)$ -th iteration stage. $\hat{\lambda}_n^{(i-1)}(t, x)$ is the resultant bit LLR corresponding to the x -th bit of $d_n(t)$ after the turbo decoding at the $(i-1)$ -th iteration stage. $\hat{H}_n^{(i)}(k)$ is given by

$$\hat{H}_n^{(i)}(k) = \sum_{m=1}^{N_t} W_{r,n,m}^{(i)}(k) \sum_{n'=1}^{N_t} H_{m,n'}(k) W_{t,n',n}(k). \quad (9)$$

N_t bit LLR sequences $\{\lambda_n^{(i)}(t, x)\}$, $n=1 \sim N_t$, are then parallel-to-serial (P/S) converted to a sequence, de-interleaved, de-punctured, and input to the turbo decoding.

2.4 Data Symbol Replica Generation

The resultant bit LLR sequence after the turbo decoding is interleaved and S/P converted to N_t sequences $\{\lambda_n^{(i)}(t, x)\}$, $n=1 \sim N_t$, to generate the time-domain soft-output data symbol replica $\{\tilde{d}_n^{(i)}(t)\}$, $n=1 \sim N_t$, which is given by

$$\tilde{d}_n^{(i)}(t) = \sum_{d \in Y} d \prod_{b_n(t,x) \in d} \Pr(b_n(t, x) | \lambda_n^{(i)}(t, x)), \quad (10)$$

where d is the data symbol candidate which has $b_n(t, x)=0$ or 1 in the data symbol set Y . $\Pr(b_n(t, x) | \lambda_n^{(i)}(t, x))$ is the *a posteriori* probability of $b_n(t, x)$ after the turbo decoding at the i -th iteration stage (i.e., when $\lambda_n^{(i)}(t, x)$ is given) given by

$$\begin{cases} \Pr(b_n(t, x) = 0 | \lambda_n^{(i)}(t, x)) = -\frac{1}{2} \tanh \left(\frac{\lambda_n^{(i)}(t, x)}{2} \right) + \frac{1}{2} \\ \Pr(b_n(t, x) = 1 | \lambda_n^{(i)}(t, x)) = \frac{1}{2} \tanh \left(\frac{\lambda_n^{(i)}(t, x)}{2} \right) + \frac{1}{2}. \end{cases} \quad (11)$$

Substituting Eq. (11), Eq. (10) is rewritten as

$$\begin{aligned} \tilde{d}_n^{(i)}(t) &= \begin{cases} \frac{1}{\sqrt{2}} \left(\tanh\left(\frac{\hat{\lambda}_n^{(i)}(t, 1)}{2}\right) + j \tanh\left(\frac{\hat{\lambda}_n^{(i)}(t, 2)}{2}\right) \right) & \text{for QPSK,} \\ \frac{1}{\sqrt{10}} \tanh\left(\frac{\hat{\lambda}_n^{(i)}(t, 1)}{2}\right) \left(2 + \tanh\left(\frac{\hat{\lambda}_n^{(i)}(t, 2)}{2}\right) \right) \\ + \frac{1}{\sqrt{10}} \tanh\left(\frac{\hat{\lambda}_n^{(i)}(t, 3)}{2}\right) \left(2 + \tanh\left(\frac{\hat{\lambda}_n^{(i)}(t, 4)}{2}\right) \right) & \text{for 16QAM} \end{cases} \end{aligned} \quad (12)$$

By using Eq.(12) and applying N_c -point DFT, the frequency-domain soft-output data symbol replica vector $\tilde{\mathbf{D}}^{(i)}(k)$ is obtained. Then, the residual ISI replica for the $(i+1)$ -th iteration is generated using $\tilde{\mathbf{D}}^{(i)}(k)$. The above steps are iterated for I times and data decision is carried out using the resultant bit LLR sequence after the turbo decoding.

3. Derivation of Tx/Rx Filters

In this section, we derive the optimal Tx and Rx filter matrices based on MMSE criterion. At first, the Rx filter matrix which minimizes the MSE described later is derived for a given Tx filter matrix. Then, a virtual MSE is defined by approximating the MSE. The derivation of the Tx matrix which minimizes the virtual MSE consists of the following 2 parts: 1) derivation of precoding matrix, 2) derivation of Tx power allocation.

The total MSE $\varepsilon^{(i)}$ of the blocks between the data symbol vector $\mathbf{D}(k)$ and the soft-output vector $\tilde{\mathbf{D}}^{(i)}(k)$ after the iterative IC at the i -th iteration stage is defined as

$$\varepsilon^{(i)} \equiv E \left[\sum_{k=1}^{N_c} \text{tr} \left\{ \left(\mathbf{D}(k) - \frac{\tilde{\mathbf{D}}^{(i)}(k)}{\sqrt{2E_s/T_s}} \right) \times \left(\mathbf{D}(k) - \frac{\tilde{\mathbf{D}}^{(i)}(k)}{\sqrt{2E_s/T_s}} \right)^H \right\} \right]. \quad (13)$$

Substituting Eq.(4) into Eq.(13), the total MSE can be rewritten as

$$\begin{aligned} \varepsilon^{(i)} &= \sum_{k=1}^{N_c} \text{tr} \left\{ \left(\mathbf{I}_{N_r} - \tilde{\mathbf{H}}^{(i)} \right) \left(\mathbf{I}_{N_r} - \tilde{\mathbf{H}}^{(i)} \right)^H \right\} \\ &+ \sum_{k=1}^{N_c} \text{tr} \left\{ \left(\tilde{\mathbf{H}}^{(i)} - \mathbf{W}_r^{(i)}(k) \mathbf{H}(k) \mathbf{W}_t(k) \right) \rho^{(i-1)} \right. \\ &\quad \left. \times \left(\tilde{\mathbf{H}}^{(i)} - \mathbf{W}_r^{(i)}(k) \mathbf{H}(k) \mathbf{W}_t(k) \right)^H \right\} \\ &+ \gamma^{-1} \sum_{k=1}^{N_c} \text{tr} \left\{ \mathbf{W}_r^{(i)}(k) \left(\mathbf{W}_r^{(i)}(k) \right)^H \right\}, \end{aligned} \quad (14)$$

where $\gamma = E_s/N_0$, and we use $E[\mathbf{D}(k)\mathbf{D}^H(k)] = \mathbf{I}_{N_r}$ and $E[\mathbf{Z}(k)\mathbf{Z}^H(k)] = (2N_0/T_s)\mathbf{I}_{N_r}$. $\rho^{(i-1)} \in \mathbb{R}^{N_r \times N_r}$ is the diagonal matrix whose (n, n) -th component $\rho_n^{(i-1)}$ is given by Eq. (8). As the number of iterations increases, the residual ISI is reduced (i.e., accuracy of the symbol replicas becomes high) and $\rho^{(i-1)}$ gets close to $\mathbf{0}_{N_r \times N_r}$.

The minimization of the total MSE $\varepsilon^{(i)}$ under the total transmit power constraint is formulated as

$$\min_{\{\mathbf{W}_t(k), \mathbf{W}_r^{(i)}(k)\}} \varepsilon^{(i)} \quad (15a)$$

$$\text{s.t.} \sum_{k=1}^{N_c} \text{tr} \left(\mathbf{W}_t(k) \mathbf{W}_t^{(i)}(k) \right) = N_c. \quad (15b)$$

The Tx and Rx filters which satisfy the above problem are the MMSE solution. However, it is quite difficult to derive a set of MMSE filter matrices $\{\mathbf{W}_{t,opt}(k), \mathbf{W}_{r,opt}^{(i)}(k)\}$ at the same time since $\mathbf{W}_t(k)$ is the function of $\mathbf{W}_r^{(i)}(k)$ or vice versa. Therefore, in this paper, as in [10], we consider the concatenation of Tx filter and MIMO channel as a equivalent channel $\bar{\mathbf{H}}(k) = \mathbf{H}(k)\mathbf{W}_t(k)$ and first, we derive the optimal Rx filter matrix $\mathbf{W}_{r,opt}^{(i)}(k)$. Then, we derive the optimal Tx filter matrix $\mathbf{W}_{t,opt}(k)$ by solving the optimization problem of Eq. (15) for the given $\mathbf{W}_{r,opt}^{(i)}(k)$.

3.1 Rx Filter

By considering $\bar{\mathbf{H}}(k) = \mathbf{H}(k)\mathbf{W}_t(k)$ as the equivalent channel matrix, the objective function $\varepsilon^{(i)}$ given as Eq. (14) becomes a convex function since the Hessian matrix $\nabla^2 \varepsilon^{(i)}$ is positive semidefinite [14]. Therefore, the $\varepsilon^{(i)}$ is minimized when $\partial \varepsilon^{(i)} / \partial \mathbf{W}_r^{(i)}(k) = 0$. As a consequence, $\mathbf{W}_{r,opt}^{(i)}(k)$ is obtained as

$$\mathbf{W}_{r,opt}^{(i)}(k) = \bar{\mathbf{H}}^H(k) \left(\bar{\mathbf{H}}(k) \rho^{(i-1)} \bar{\mathbf{H}}^H(k) + \gamma^{-1} \mathbf{I}_{N_r} \right)^{-1}. \quad (16)$$

3.2 Tx Filter

From the previous subsection, it can be understood that the Rx filter is updated in each iteration stage since it includes $\rho^{(i-1)}$ as seen in Eq. (16). As the number of iterations increases, $\rho^{(i-1)}$ gets close to $\mathbf{0}_{N_r \times N_r}$ and $\mathbf{W}_{r,opt}^{(i)}(k)$ approaches the maximal-ratio combining (MRC) based filter $\gamma \bar{\mathbf{H}}^H(k)$. This Rx filter maximizes the frequency diversity gain.

In contrast to the Rx filter, Tx filter cannot be updated. In [10], we derived the Tx filter matrix for a given Rx filter matrix. However, the previously proposed Tx filter matrix does not take into account the iterative IC at the receiver. If the iterative IC at the receiver is taken into account at the transmitter, Tx filtering can provide a much higher frequency diversity gain than the previous one.

In this paper, in order to derive the optimal Tx filter matrix $\mathbf{W}_{t,opt}(k)$, we assume a virtual Rx filter matrix $\mathbf{W}_r^{\text{Tx}}(k) \in \mathbb{C}^{N_r \times N_r}$ as

$$\mathbf{W}_r^{\text{Tx}}(k) = \bar{\mathbf{H}}^H(k) \left(\bar{\mathbf{H}}(k) \rho^{\text{Tx}} \bar{\mathbf{H}}^H(k) + \gamma^{-1} \mathbf{I}_{N_r} \right)^{-1}, \quad (17)$$

where $\rho^{\text{Tx}} \in \mathbb{R}^{N_r \times N_r}$ is the diagonal matrix whose (n, n) -th component ρ_n^{Tx} is a virtual coefficient which is a parameter between 0 to 1. The virtual total MSE ε^{Tx} is given by replacing $\tilde{\mathbf{H}}^{(i)}$ with \mathbf{I}_{N_r} as

$$\begin{aligned} \varepsilon^{\text{Tx}} = & \sum_{k=1}^{N_c} \text{tr} \left\{ \left(\mathbf{I}_{N_r} - \mathbf{W}_r^{\text{Tx}}(k) \mathbf{H}(k) \mathbf{W}_t(k) \right) \boldsymbol{\rho}^{\text{Tx}} \right\} \\ & \times \left(\mathbf{I}_{N_r} - \mathbf{W}_r^{\text{Tx}}(k) \mathbf{H}(k) \mathbf{W}_t(k) \right)^H \\ & + \gamma^{-1} \sum_{k=1}^{N_c} \text{tr} \left\{ \mathbf{W}_r^{\text{Tx}}(k) \left(\mathbf{W}_r^{\text{Tx}}(k) \right)^H \right\}, \end{aligned} \quad (18)$$

and we solve the virtual optimization problem as

$$\begin{aligned} \min_{\{\mathbf{W}_t(k)\}} \varepsilon^{\text{Tx}} \quad (19) \\ \text{s.t. (15b).} \end{aligned}$$

The objective function ε^{Tx} is expressed as the function only of the Tx filter matrix $\mathbf{W}_t(k)$ by substituting $\mathbf{W}_r^{\text{Tx}}(k)$ into ε^{Tx} . ε^{Tx} is rewritten by substituting Eq. (17) into Eq. (18) and using the matrix inversion lemma [15] as

$$\varepsilon^{\text{Tx}} = \sum_{k=1}^{N_c} \text{tr} \left(\gamma \mathbf{W}_t^H(k) \mathbf{H}^H(k) \mathbf{H}(k) \mathbf{W}_t(k) \boldsymbol{\rho}^{\text{Tx}} + \mathbf{I}_{N_r} \right)^{-1}. \quad (20)$$

For any $X \times X$ positive semidefinite Hermitian matrix \mathbf{X} , it is true that $\text{tr}[\mathbf{X}] = \sum_{x=1}^X \xi_x$, where ξ_x is the $x(=1 \sim X)$ -th eigenvalue of \mathbf{X} [15]. Therefore, Eq. (20) can be rewritten as

$$\begin{aligned} \varepsilon^{\text{Tx}} &= \sum_{k=1}^{N_c} \text{tr} \left(\gamma \boldsymbol{\rho}^{\text{Tx}} \mathbf{W}_t^H(k) \mathbf{W}_t(k) \mathbf{H}^H(k) \mathbf{H}(k) + \mathbf{I}_{N_r} \right)^{-1} \\ &= \sum_{k=1}^{N_c} \sum_{n=1}^{N_r} \left(\gamma \rho_n^{\text{Tx}} P_n(k) \Lambda_n(k) + 1 \right)^{-1}. \end{aligned} \quad (21)$$

Here, we use $\text{tr}[\mathbf{A}\mathbf{B}] = \text{tr}[\mathbf{B}\mathbf{A}]$ with $\mathbf{A} \in \mathbb{C}^{A \times B}$ and $\mathbf{B} \in \mathbb{C}^{B \times A}$. $P_n(k)$ and $\Lambda_n(k)$ are the n -th eigenvalues of $\mathbf{W}_t^H(k) \mathbf{W}_t(k)$ and $\mathbf{H}^H(k) \mathbf{H}(k)$, respectively.

$\mathbf{H}(k)$ and $\mathbf{W}_t(k)$ can be transformed by singular value decomposition [15] as

$$\begin{cases} \mathbf{H}(k) = \mathbf{U}_h(k) \sqrt{\boldsymbol{\Lambda}(k)} \mathbf{V}_h^H(k) \\ \mathbf{W}_t(k) = \mathbf{U}_t(k) \sqrt{\mathbf{P}(k)} \mathbf{V}_t^H(k) \end{cases}, \quad (22)$$

where $\mathbf{U}_h(k) \in \mathbb{C}^{N_r \times N_r}$, $\mathbf{V}_h(k) \in \mathbb{C}^{N_r \times N_r}$, $\mathbf{U}_t(k) \in \mathbb{C}^{N_r \times N_r}$, and $\mathbf{V}_t(k) \in \mathbb{C}^{N_r \times N_r}$ are respectively unitary matrices. $\boldsymbol{\Lambda}(k) \in \mathbb{R}^{N_r \times N_r}$ is the matrix whose (n, n) -th element is $\Lambda_n(k)$, and any other elements are zero. $\mathbf{P}(k) \in \mathbb{R}^{N_r \times N_r}$ is the diagonal matrix whose (n, n) -th element is $P_n(k)$. Therefore Eq. (20) can also be rewritten by substituting Eq. (22) as

$$\varepsilon^{\text{Tx}} = \sum_{k=1}^{N_c} \text{tr} \left\{ \gamma \boldsymbol{\rho}^{\text{Tx}} \sqrt{\mathbf{P}(k)} \mathbf{U}_t^H(k) \mathbf{V}_h(k) \sqrt{\boldsymbol{\Lambda}^T(k)} \right\}^{-1} \times \left\{ \sqrt{\boldsymbol{\Lambda}(k)} \mathbf{V}_h^H(k) \mathbf{U}_t(k) \sqrt{\mathbf{P}(k)} + \mathbf{I}_{N_r} \right\}. \quad (23)$$

Since Eq. (23) is equal to Eq. (21), $\mathbf{U}_t(k) = \mathbf{V}_h(k)$. Furthermore, $\mathbf{V}_t(k)$ does not appear in Eq. (23) since $\mathbf{V}_t(k) \mathbf{V}_t^H(k) = \mathbf{V}_t^H(k) \mathbf{V}_t(k) = \mathbf{I}_{N_r}$ due to the property of unitary

matrix. Therefore, the optimization problem does not depend on $\mathbf{V}_t(k)$. Accordingly, $\mathbf{V}_t(k)$ can be set to an arbitrary $N_r \times N_r$ unitary matrix for all k . In this paper, we set $\mathbf{V}_{t,opt}(k) = \mathbf{I}_{N_r}$ for the sake of brevity, but the PAPR of the transmit signal can be reduced by appropriately setting $\mathbf{V}_t(k)$. As a consequence, $\mathbf{W}_{t,opt}(k)$ is expressed as

$$\mathbf{W}_{t,opt}(k) = \mathbf{V}_h(k) \sqrt{\mathbf{P}_{opt}(k)}. \quad (24)$$

The optimization problem is rewritten by substituting Eq. (24) into Eq. (20) as

$$\min_{\{P_n(k)\}} \sum_{k=1}^{N_c} \sum_{n=1}^{N_r} \left(\gamma \rho_n^{\text{Tx}} P_n(k) \Lambda_n(k) + 1 \right)^{-1} \quad (25a)$$

$$\text{s.t. } \sum_{k=1}^{N_c} \sum_{n=1}^{N_r} P_n(k) = N_c \quad (25b)$$

$$P_n(k) \geq 0, \forall n, k \quad (25c)$$

which can be solved by non-linear programming and the solution satisfies Karush-Kuhn-Tucker (KKT) condition [14]. Following [14], the optimal solution is given by

$$P_{n,opt}(k) = \left(\frac{1}{\sqrt{\mu}} \frac{1}{\sqrt{\gamma \Lambda_n(k)}} - \frac{1}{\gamma \rho_n^{\text{Tx}} \Lambda_n(k)} \right)^+, \quad (26)$$

where μ is chosen to satisfy the constraint conditions of Eqs. (25b) and (25c).

3.3 Discussion

In this subsection, we discuss the behavior of joint Tx/Rx MMSE filtering and iterative IC. The equivalent channel matrix $\hat{\mathbf{H}}^{(i)}(k)$ after the Rx MMSE filtering at the i -th iteration stage is expressed as

$$\begin{aligned} \hat{\mathbf{H}}^{(i)}(k) &= \mathbf{W}_{r,opt}^{(i)}(k) \mathbf{H}(k) \mathbf{W}_{t,opt}(k) \\ &= \text{diag} \left[\hat{H}_1^{(i)}(k) \cdots \hat{H}_{N_r}^{(i)}(k) \right] \\ &= \text{diag} \left[\frac{P_{1,opt}(k) \Lambda_1(k)}{\rho_1^{(i-1)} P_{1,opt}(k) \Lambda_1(k) + \gamma^{-1}} \cdots \right. \\ &\quad \left. \frac{P_{N_r,opt}(k) \Lambda_{N_r}(k)}{\rho_{N_r}^{(i-1)} P_{N_r,opt}(k) \Lambda_{N_r}(k) + \gamma^{-1}} \right]. \end{aligned} \quad (27)$$

It can be seen from Eq. (27) that the MIMO channel matrix $\mathbf{H}(k)$ is diagonalized (i.e., IAI is removed) by joint Tx/Rx MMSE filtering. In addition, ISI can be significantly suppressed by applying the MMSE based Tx power allocation following Eq. (26) and Rx FDE to each eigenmode taking into account the iterative IC.

Figure 2 shows one shot observation of the proposed MMSE power allocation for $\rho_1^{\text{Tx}} = \rho_2^{\text{Tx}} = 1.0, 0.5$, and 0.1 when $N_r = N_r = 2$, $N_c = 128$, $\gamma = 10$ dB, and a 16-path frequency-selective block Rayleigh fading having uniform power delay profile without fading correlation. It can be understood from Eq. (26) that the proposed MMSE power

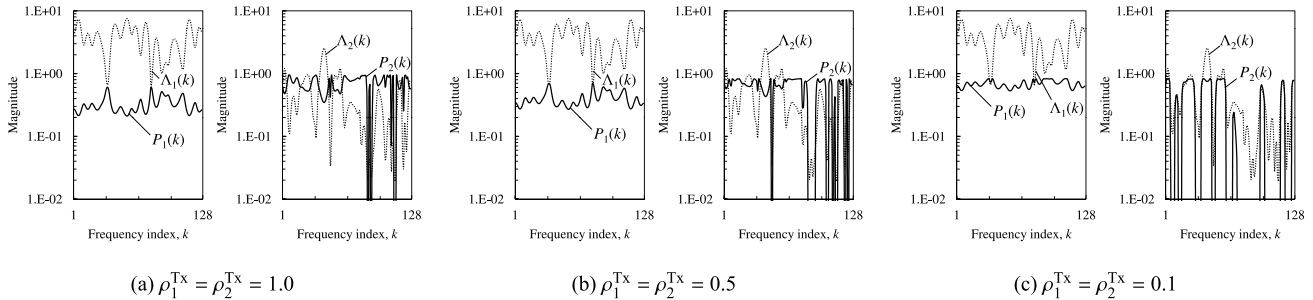


Fig. 2 One shot observation of MMSE power allocation.

allocation depends on the parameter ρ_n^{Tx} which indicates the reliability of the iterative IC assumed at the transmitter. If the transmitter assumes the iterative IC cannot suppress ISI on the n -th eigenmode at all, ρ_n^{Tx} is set to 1.0 (i.e., Fig. 2(a)). In this case, the transmitter allocates power to suppress ISI (i.e., frequency-selectivity) by itself not only on the 1st eigenmode but also the 2nd eigenmode. On the other hand, if the transmitter assumes the iterative IC can sufficiently suppress ISI on the n -th eigenmode, ρ_n^{Tx} is set to small (i.e., Fig. 2(c)). In this case, the transmitter allocates no power to the frequencies which have low eigenvalues especially on the 2nd eigenmode but allocates much power to the frequencies which have high eigenvalues to improve the received signal-to-noise power ratio (SNR). It is quite difficult to analytically derive the optimal ρ^{Tx} because it depends on the data modulation level, channel coding scheme, average transmit E_s/N_0 , γ , instantaneous channel gain, the number of iterations of IC, and so on. Therefore, in this paper, the optimal ρ^{Tx} is found by computer simulation such that the average BER is minimized for a given γ . The impact of ρ^{Tx} on BER performance is discussed in the next section.

4. Computer Simulation

4.1 Computer Simulation Condition

Computer simulation condition is summarized in Table 1. A turbo encoder with the original coding rate 1/3 using two (13,15) recursive systematic convolutional (RSC) encoders, a random interleaver/deinterleaver, and log maximum *a posteriori* probability (MAP) turbo decoding with only 1 iteration (i.e., only 1 iteration is carried out in the inner loop (between two MAP component decoders in turbo decoder)) are used. The codeword length $K=1024$ bits with coding rate $R_{\text{code}}=1/2$ or $3/4$. The channel is assumed to be a 16-path frequency-selective block Rayleigh fading having uniform power delay profile. Uncorrelated fading and ideal channel estimation at both transmitter and receiver are assumed.

4.2 Impact of ρ^{Tx} on BER Performance

Figure 3 shows the average BER performance of SC-MIMO transmission using iterative IC with the proposed joint

Table 1 Computer simulation condition.

Parameter	Value
No. of coded bits	$K=1024$
Data modulation	QPSK, 16QAM
No. of DFT/IDFT points	$N_c=128$
Guard interval length	$N_g=16$
No. of Tx/Rx antennas	$(N_t, N_r)=(2, 2)$
Fading type	Frequency-selective block Rayleigh
Power delay profile	16-path uniform
Fading correlation	Uncorrelated
Channel estimation	Ideal

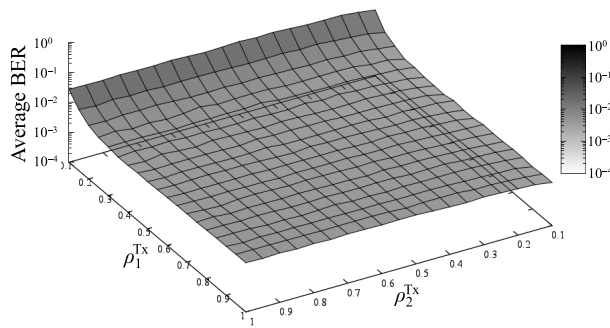
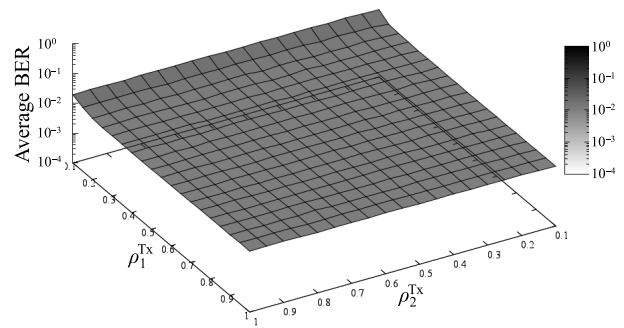
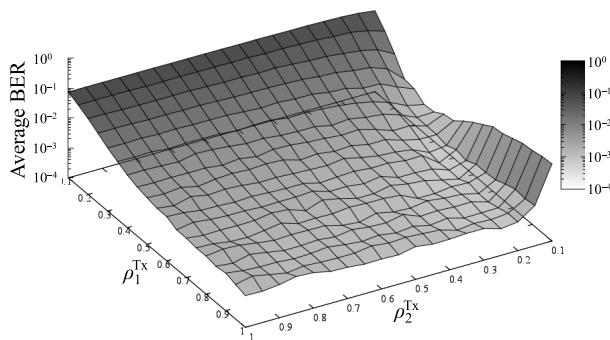
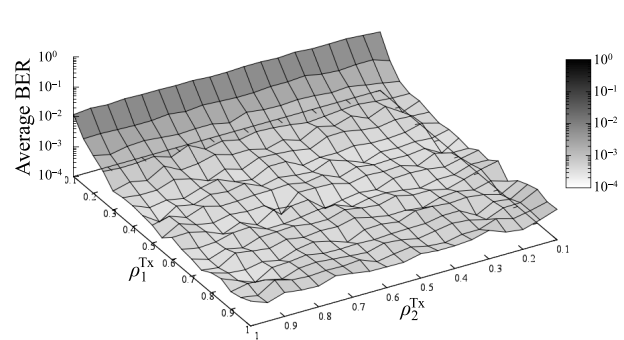
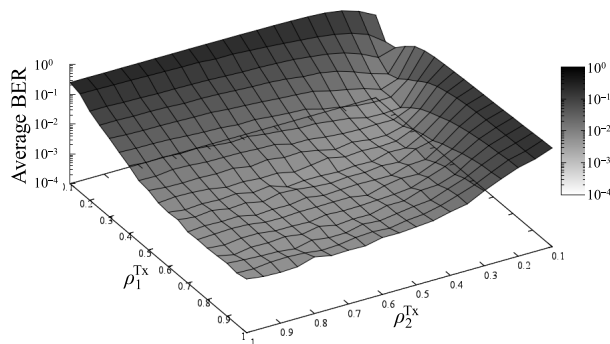
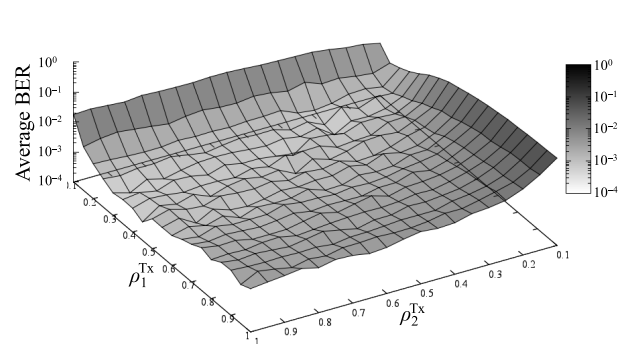
Tx/Rx MMSE filtering for various values of ρ^{Tx} . Here, average transmit bit energy-to-noise power spectrum density ratio $E_b/N_0=(E_s/N_0)(1+N_g/N_c)/(R_{\text{code}} \log_2 M)$.

It is seen from Figs. 3(a) and (b) that, in uncoded case, the impact of ρ^{Tx} on BER performance is not significant except for the case of quite small ρ_2^{Tx} . In other words, ρ_1^{Tx} does not affect BER performance but ρ_2^{Tx} limits the overall performance improvement. In uncoded case, symbol replicas of each eigenmode are generated from the received signal on each eigenmode itself. Therefore, symbol replicas on 1st eigenmode (higher eigenvalue) can be generated with high accuracy but those on 2nd eigenmode (lower eigenvalue) cannot. As a consequence, setting ρ_2^{Tx} quite small directly leads to the degradation of overall BER performance.

On the other hand, it is seen from Figs. 3(c) to (f) that, in turbo coded case, the impact of ρ^{Tx} on BER performance is significant. In turbo coded case, symbol replicas of each eigenmode are generated from the resultant bit LLR sequence after the turbo decoding. The resultant bit LLR sequence is calculated from the received signals on all eigenmodes through interleaver/deinterleaver and is used for generating the symbol replicas on all eigenmodes. Therefore, ρ_1^{Tx} affects not only the accuracy of symbol replicas on 1st eigenmode but also that on 2nd eigenmode and vice versa. As a consequence, both ρ_1^{Tx} and ρ_2^{Tx} affect the BER performance.

4.3 Comparison with Conventional Rx MMSE Filtering

Figure 4 shows the average BER performance of SC-MIMO transmission using iterative IC with the proposed joint

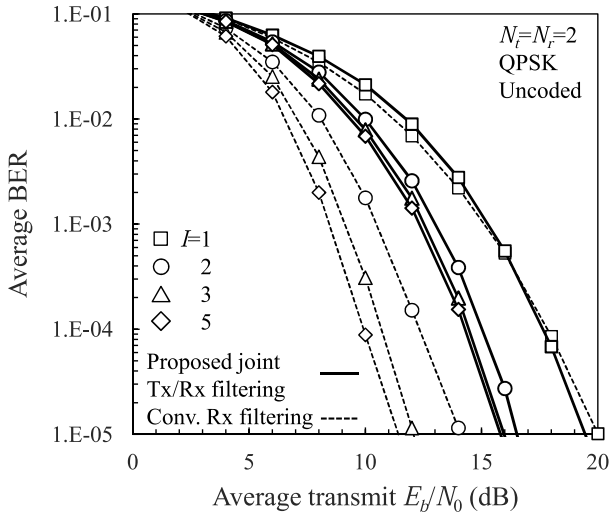
(a) Uncoded, QPSK, average transmit $E_b/N_0=14$ (dB), $I=5$ (b) Uncoded, 16QAM, average transmit $E_b/N_0=20$ (dB), $I=5$ (c) $R_{code}=3/4$ turbo coded, QPSK, average transmit $E_b/N_0=8$ (dB), $I=5$ (d) $R_{code}=3/4$ turbo coded, 16QAM, average transmit $E_b/N_0=(dB)$, $I=5$ (e) $R_{code}=1/2$ turbo coded, QPSK, average transmit $E_b/N_0=6$ (dB), $I=5$ (f) $R_{code}=1/2$ turbo coded, 16QAM, average transmit $E_b/N_0=8$ (dB), $I=5$ **Fig. 3** Impact of ρ^{Tx} on BER.

Tx/Rx MMSE filtering for various numbers I of iterations. The average BER performance with conventional Rx filtering is also shown for comparison.

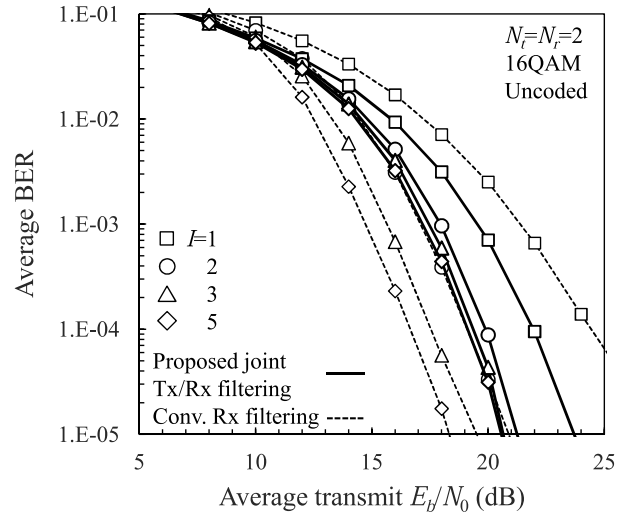
It is seen from Figs. 4(a) and (b) that, in uncoded case, the proposed joint Tx/Rx MMSE filtering has worse average BER performance than the conventional Rx MMSE filtering assuming the same number I of iterations except for the case when $I=1$ (i.e., without iterative IC). The reason for this degraded performance in the uncoded case is discussed below. All received soft-output symbols have almost the same reliability when Rx filtering is used. However, there

exists a large received quality gap among eigenmodes when joint Tx/Rx filtering is used. This is because the eigenvalues of each eigenmode (i.e., equivalent channel gain) are quite different from each other as mentioned in Sect. 4.2. Therefore, the accuracy of the symbol replicas whose symbols are transmitted through the eigenmode having low eigenvalue is low and cannot be improved even using iterative IC. This problem can be regarded as a kind of burst error.

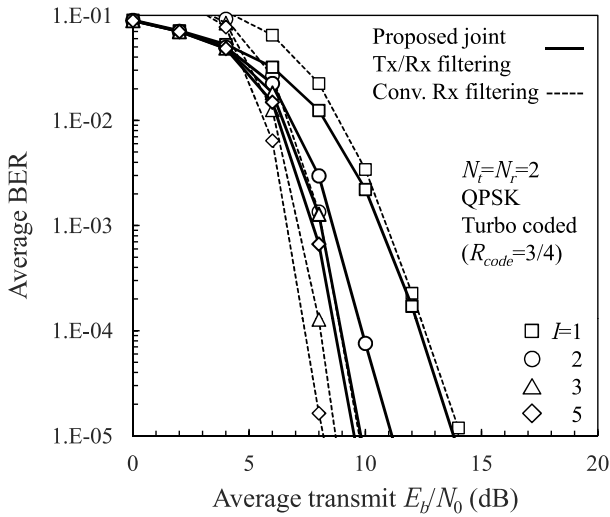
On the other hand, it is seen from Figs. 4(e) and (f) that, when turbo coding with $R_{code}=1/2$ is used, the proposed joint Tx/Rx filtering has better average BER performance



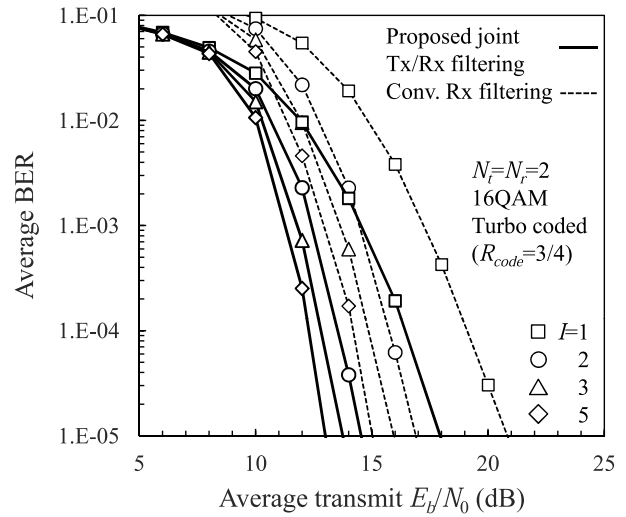
(a) Uncoded, QPSK



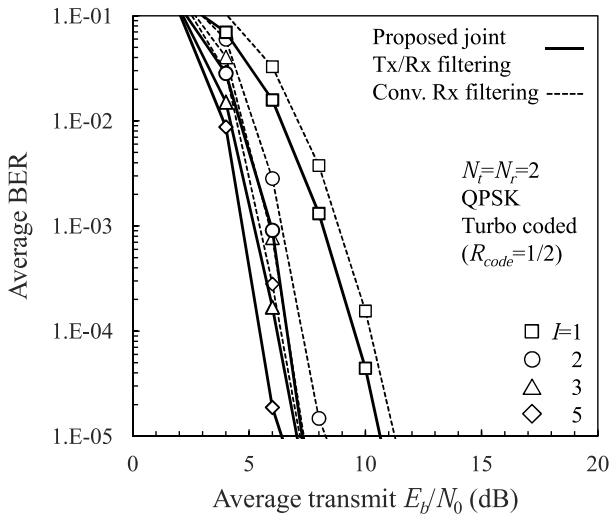
(b) Uncoded, 16QAM



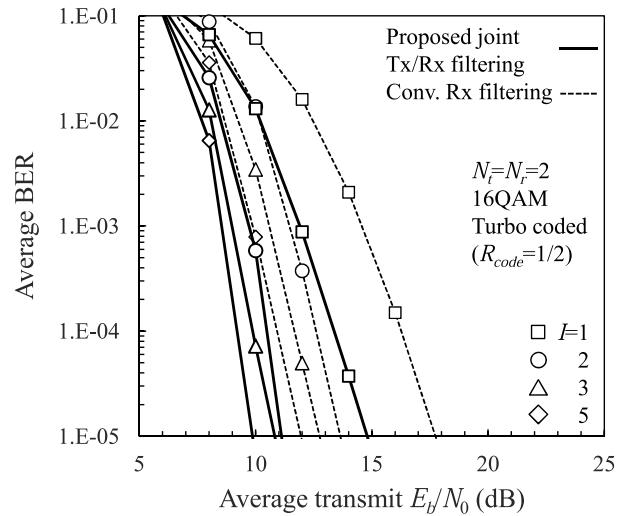
(c) $R_{code}=3/4$ turbo coded, QPSK



(d) $R_{code}=3/4$ turbo coded, 16QAM



(e) $R_{code}=1/2$ turbo coded, QPSK



(f) $R_{code}=1/2$ turbo coded, 16QAM

Fig. 4 Comparison with conventional Rx MMSE filtering.

than the conventional Rx filtering. This is because the burst error occurring on the eigenmode having low received quality is randomized by randomizing the systematic bits and parity bits, which are generated at the turbo encoder, at the channel interleaver. Therefore, the accuracy of the symbol replicas can be improved by the iterative IC and turbo decoding and the average BER performance is significantly improved as mentioned in Sect. 4.2.

It can also be seen from Fig. 4 that the proposed joint Tx/Rx filtering produces more improvement when the modulation level becomes higher. This is because bigger BER performance improvement is obtained by the received signal-to-interference plus noise power ratio (SINR) improvement when higher modulation level is used (i.e., the Euclidean distance between symbols is smaller).

Below, based on the above observation, we will discuss about the BER performance achievable by the proposed method when turbo coding with $R_{code}=3/4$ is used (Figs. 4(c) and (d)). It is seen from Fig. 4(c) that, in the case of QPSK, the proposed joint Tx/Rx filtering has slightly worse average BER performance than the conventional Rx filtering. This slight performance degradation is because the burst error occurring on the eigenmode having low received quality cannot be sufficiently randomized by the channel interleaver since the coding rate is not sufficiently low. On the other hand, it is seen from Fig. 4(d) that, in the case of 16QAM, the proposed joint Tx/Rx filtering has better average BER performance than the conventional Rx filtering. This is because bigger BER performance improvement is obtained by the received SINR improvement in the case of 16QAM than in the case of QPSK.

5. Conclusion

In this paper, we proposed a new joint Tx/Rx MMSE filtering for SC-MIMO eigenmode transmission using iterative IC and newly derived the optimal Tx/Rx filters in closed-forms. The proposed joint Tx/Rx MMSE filtering transforms the MIMO channel into eigenmodes to remove IAI and applies MMSE based frequency-domain Tx power allocation and Rx FDE to each eigenmode to further suppress the residual ISI taking into account the iterative IC at the receiver. We showed, by computer simulation, that joint Tx/Rx MMSE filtering can significantly improve the average BER performance of turbo coded SC-MIMO transmission using iterative IC.

References

- [1] E. Biglieri, R. Calderbank, A. Constantinides, A. Goldsmith, A. Paulraj, and H.V. Poor, *MIMO Wireless Communications*, Cambridge University Press, 2007.
- [2] G.L. Stuber, J.R. Barry, S.W. McLaughlin, Y. Li, M.A. Ingram, and T.G. Pratt, "Broadband MIMO-OFDM wireless communications," *Proc. IEEE*, vol.92, no.2, pp.271–294, 2004.
- [3] Y.-L. Lee, Y.-H. You, W.-G. Jeon, J.-H. Paik, and H.-K. Song, "Peak-to-average power ratio in MIMO-OFDM systems using selective mapping," *IEEE Commun. Lett.*, vol.7, no.12, pp.575–577, Dec. 2003.

- [4] D. Tse and P. Viswanath, *Fundamentals of Wireless Communication*, Cambridge University Press, 2005.
- [5] S. Han and J. Lee, "An overview of peak-to-average power ratio reduction techniques for multicarrier transmission," *IEEE Wireless Commun. Mag.*, vol.12, no.2, pp.56–65, April 2005.
- [6] J.P. Coon and M.A. Beach, "An investigation of MIMO single-carrier frequency-domain MMSE equalization," *London Communications Symposium*, pp.237–240, 2002.
- [7] S. Okuyama, T. Yamamoto, K. Takeda, and F. Adachi, "Iterative MMSE detection with interference cancellation for up-link HARQ using frequency-domain filtered SC-FDMA MIMO multiplexing," *IEICE Trans. Commun.*, vol.E94-B, no.12, pp.3559–3568, Dec. 2011.
- [8] A. Nakajima and F. Adachi, "Iterative FDIC using 2D-MMSE FDE for turbo-coded HARQ in SC-MIMO multiplexing," *IEICE Trans. Commun.*, vol.E90-B, no.3, pp.693–695, March 2007.
- [9] K. Nagatomi, H. Kawai, and K. Higuchi, "Complexity-reduced MLD based on QR decomposition in OFDM MIMO multiplexing with frequency domain spreading and code multiplexing," *EURASIP J. Advances in Signal Processing*, vol.2011, no.1, 525829, Jan. 2011.
- [10] S. Kumagai, T. Obara, T. Yamamoto, and F. Adachi, "Joint Tx/Rx MMSE filtering for single-carrier MIMO transmission," *IEICE Trans. Commun.*, vol.E97-B, no.9, pp.1967–1976, Sept. 2014.
- [11] K. Ishihara, K. Takeda, and F. Adachi, "Iterative frequency-domain soft interference cancellation for multicode DS- and MC-CDMA transmissions and performance comparison," *IEICE Trans. Commun.*, vol.E89-B, no.12, pp.3344–3355, Dec. 2006.
- [12] N. Benvenuto and S. Tomasin, "Iterative design and detection of a DFE in the frequency domain," *IEEE Trans. Commun.*, vol.53, no.11, pp.1867–1875, Nov. 2005.
- [13] N. Benvenuto, R. Dinis, D. Falconer, and S. Tomasin, "Single carrier modulation with nonlinear frequency domain equalization: An idea whose time has come — Again," *Proc. IEEE*, vol.98, no.1, pp.69–96, 2010.
- [14] S. Boyd and L. Vandenberghe, *Convex Optimization*, Cambridge University Press, 2006.
- [15] R.A. Horn and C.R. Johnson, *Matrix Analysis*, Cambridge University Press, 1985.



Shinya Kumagai received his B.E. degree in Information and Intelligent Systems in 2011 and M.E. degree in Electrical and Communications engineering in 2013, respectively, from Tohoku University, Sendai, Japan. Currently, he is a Japan Society for the Promotion of Science (JSPS) research fellow, studying toward his Ph.D. degree at the Department of Communications Engineering, Graduate School of Engineering, Tohoku University. His research interests include channel equalization and multiple-

input multiple-output (MIMO) transmission techniques for mobile communication systems. He was a recipient of the 2012 IEICE RCS (Radio Communication Systems) Outstanding Research Award.



FumiYuki Adachi received the B.S. and Dr. Eng. degrees in electrical engineering from Tohoku University, Sendai, Japan, in 1973 and 1984, respectively. In April 1973, he joined the Electrical Communications Laboratories of Nippon Telegraph & Telephone Corporation (now NTT) and conducted various types of research related to digital cellular mobile communications. From July 1992 to December 1999, he was with NTT Mobile Communications Network, Inc. (now NTT DoCoMo, Inc.), where he

led a research group on wideband/broadband CDMA wireless access for IMT-2000 and beyond. Since January 2000, he has been with Tohoku University, Sendai, Japan, where he is a Professor of Communications Engineering at the Graduate School of Engineering. In 2011, he was appointed a Distinguished Professor. His research interests are in the areas of wireless signal processing and networking including broadband wireless access, equalization, transmit/receive antenna diversity, MIMO, adaptive transmission, and channel coding, etc. From October 1984 to September 1985, he was a United Kingdom SERC Visiting Research Fellow in the Department of Electrical Engineering and Electronics at Liverpool University. Dr. Adachi is an IEEE fellow and a VTS Distinguished Lecturer for 2011 to 2013. He was a co-recipient of the IEEE Vehicular Technology Transactions best paper of the year award 1980 and again 1990 and also a recipient of Avant Garde award 2000. He was a recipient of Thomson Scientific Research Front Award 2004 and Ericsson Telecommunications Award 2008, Telecom System Technology Award 2009, and Prime Minister Invention Prize 2010.